Dalton Transactions

COMMUNICATION

View Article Online
View Journal | View Issue

Check for updates

Cite this: *Dalton Trans.*, 2017, **46**, 5133

Received 7th January 2017,
Accepted 16th March 2017

DOI: 10.1039/c7dt00058h

rsc.li/dalton

Open Access Article. Published on 17 March 2017. Downloaded on 1/18/2026 6:30:33 PM.
This article is licensed under a Creative Commons Attribution 3.0 Unported Licence.

Magnetically recoverable Fe_3O_4@Au-coated nanoscale catalysts for the A^3-coupling reaction†

Alaa M. Munshi,[a] Mingwen Shi,[a] Sajesh P. Thomas,[a] Martin Saunders,[b] Mark A. Spackman,[a] K. Swaminathan Iyer *[a] and Nicole M. Smith*[a]

The utility of novel Fe_3O_4@Au nanoparticles as magnetically separable and recyclable heterogeneous catalysts for the A^3-coupling reaction of aldehydes, amines and terminal alkynes to yield the corresponding propargylamines is demonstrated. Herein we present a comprehensive analysis of the experimentally observed trends in the conversions with computational analysis using LUMO density on molecular isosurfaces and the electrostatic potential (ESP) effects estimated using DFT calculations.

Propargylamines are essential building blocks for biologically active compounds and are crucial intermediates in the production of pharmaceuticals and natural products.[1–3] The three-component coupling (A^3-coupling) reaction of an aldehyde, an amine and a terminal alkyne with a transition metal catalyst for C–H bond activation is considered superior to traditional methods such as nucleophilic addition of Grignard reagents or lithium acetylides to imines, which involve multistep synthesis/purification and the use of moisture sensitive agents in a regulated reaction condition.[4,5] Various homogeneous and heterogeneous metal catalysts have been reported for A^3-coupling reactions, which include gold, silver, copper and iron salts as well as gold and iridium complexes that exhibit high catalytic activity and ease of optimisation.[6–11] However, these suffer from the difficulty in separating the catalysts from the reaction mixture which in turn results in multistep purification.[12] Colloidal nanocatalysts have emerged as a particularly desirable alternative as they operate at the intersection of homogeneous and heterogeneous catalysis. They are similar to homogeneous catalysts in their accessibility and large surface area and mimic heterogeneous catalysts regarding durability and recyclability.[13] In addition, the size, shape and composition of metal nanocatalysts can be controlled by tuning their unique properties. Furthermore, integration of metal nanocatalysts with catalyst supports such as metal oxides or porous and carbonaceous materials, offer the possibility of green and sustainable catalysis.[14,15] Among the various metal nanocatalysts that have been investigated for A^3-coupling reactions, Au nanoparticles are considered the most effective due to their ability to activate the alkyne C–H bonds in the A^3-coupling reaction.[16] Following the report by Kidwai *et al.* on the use of Au nanoparticles as a catalyst for A^3-coupling reaction, significant research has been pursued with the aim of preventing aggregation of the catalyst nanoparticles.[17] Datta *et al.* developed a novel catalyst by embedding Au nanoparticles in mesoporous carbon nitride, to prevent the agglomeration of Au nanoparticles.[18] More recently, Abahmane *et al.* reported a promising catalyst comprising two Au nanocatalysts supported on alumina supports.[19]

Magnetic nanoparticles such as magnetite (Fe_3O_4) are an interesting class of catalyst supports over conventional non-magnetic colloidal systems, which enable facile separation of the nanocatalyst from the reaction mixture using an external magnetic field.[20,21] Furthermore, core–shell nanostructures have a substantial effect in the catalysis of various reactions.[22] Thus different approaches have been developed to generate core–shell nanocatalysts, with diameters ranging from 100 to 240 nm, such as Au@CeO_2 nanocomposites,[23] Au@SiO_2 nanoparticles,[24,25] Ag@Fe_3O_4 nanocomposites,[26] Fe_3O_4@MgAl-layered double hydroxides (LDH)@Au nanoparticles[27] and Au/Fe_3O_4@polydopamine (PDA) nanoparticles.[28] Herein, we report a catalyst system comprising a superparamagnetic Fe_3O_4 nanoparticle core coated with Au (Fe_3O_4@Au) for use as a catalyst in propargylamine synthesis *via* the A^3-coupling reaction. We demonstrate that this catalyst has excellent recyclability and permits ease of separation from the reaction mixture using an external magnetic field. Finally, we discuss the correlation between the selected aldehyde structures, electron density distribution, Lowest Unoccupied Molecular Orbital (LUMO) density and the electrostatic potential (ESP) at the reaction sites on molecular isosurfaces and the corresponding

[a]*School of Molecular Sciences, The University of Western Australia, Crawley, Western Australia, Australia. E-mail: swaminatha.iyer@uwa.edu.au, nicole.smith@uwa.edu.au*
[b]*Centre for Microscopy, Characterisation & Analysis, The University of Western Australia, Australia*

†Electronic supplementary information (ESI) available: Nanoparticle synthesis, characterisation details. Elements mapping data of the catalyst and TEM analysis of the catalyst. See DOI: 10.1039/c7dt00058h

Open Access Article. Published on 17 March 2017. Downloaded on 1/18/2026 6:30:33 PM.
This article is licensed under a Creative Commons Attribution 3.0 Unported Licence.

conversions using DFT calculations performed on the aldehyde reactants.

Fe_3O_4@Au nanoparticles with sizes of 100 ± 2 nm (average ± standard error mean) were fabricated in a multistep assembly process (described in ESI†).[29] Briefly, stable core Fe_3O_4–PEI (polyethyleneimine) nanoparticles were formed with sizes of 88 ± 2 nm (Fig. 1A). To facilitate the Au shell formation, the Fe_3O_4 nanoparticles were first decorated with 2 nm Au seeds (Fig. 1B and C), followed by Au shell formation. The formation of uniform Au-coated Fe_3O_4 nanoparticles was validated using transmission electron microscopy (TEM) and energy-dispersive X-ray spectroscopy (EDS) (Fig. 1D, E and ESI Fig. S1†).

The reaction medium plays a crucial role in the A^3-coupling reaction; hence, a variety of solvents (methanol, chloroform, water and acetonitrile) were screened to optimise the catalytic activity of the Fe_3O_4@Au nanoparticles (ESI, Table S1†).[17] The A^3-coupling reaction of benzaldehyde (1 mmol), piperidine (1 mmol) and phenylacetylene (1 mmol) was initially performed with 10 mol% Fe_3O_4@Au nanoparticles as the catalyst under a nitrogen atmosphere using above-mentioned solvents. Among the solvents tested, an excellent conversion of 70% (determined by ^{1}H NMR analysis) was observed in toluene at 100 °C after 24 h. The overall optimised conditions were determined to be in toluene at 100 °C for 48 h, which gave a conversion of 94% for this reaction. We note that in the absence of Fe_3O_4@Au nanoparticles, no benzaldehyde conversion was observed and poor conversion results were obtained when Au or Fe_3O_4 nanoparticles (7% and 32% respectively) were used independently as catalysts compared to Fe_3O_4@Au nanoparticles as reported in our previous study.[30] We next evaluated the recyclability of the Fe_3O_4@Au nanoparticles under the optimised conditions for up to five successive runs. After each run, the catalyst was separated using an external magnet and washed with toluene and acetone, then air dried for reuse without further purification. For the first four cycles, the loss of activity was negligible (Fig. 2), while after the fifth cycle, there was a slight reduction of 13% from the initial catalytic efficiency. This decrease could possibly be attributed to leaching of the catalyst, as indicated by ICP (Inductively Coupled Plasma) analysis (ESI†).

With the optimised conditions, we next examined the scope of the A^3-coupling reaction for various aldehydes with piperidine and phenylacetylene (Table 1). Formaldehyde and benzaldehyde showed high conversion (95% and 94% respectively) (Table 1, entries 1 and 2). In the case of 1-naphthaldehyde (Table 1, entry 3) the lower conversion (28%) relative to benzaldehyde can be attributed to the bulkier substituent. Furthermore, 4-methoxybenzaldehyde (Table 1, entry 5) resulted in a lower conversion (25%) compared to 4-methylbenzaldehyde (63%) (Table 1, entry 4). This can be due to the stronger electron donating resonance effect and increased bulkiness of the methoxy (–OCH_3) substituent at the *para* position relative to the latter with a methyl (–CH_3) substituent. Similarly, 4-chlorobenzaldehyde (Table 1, entry 7) had a lower

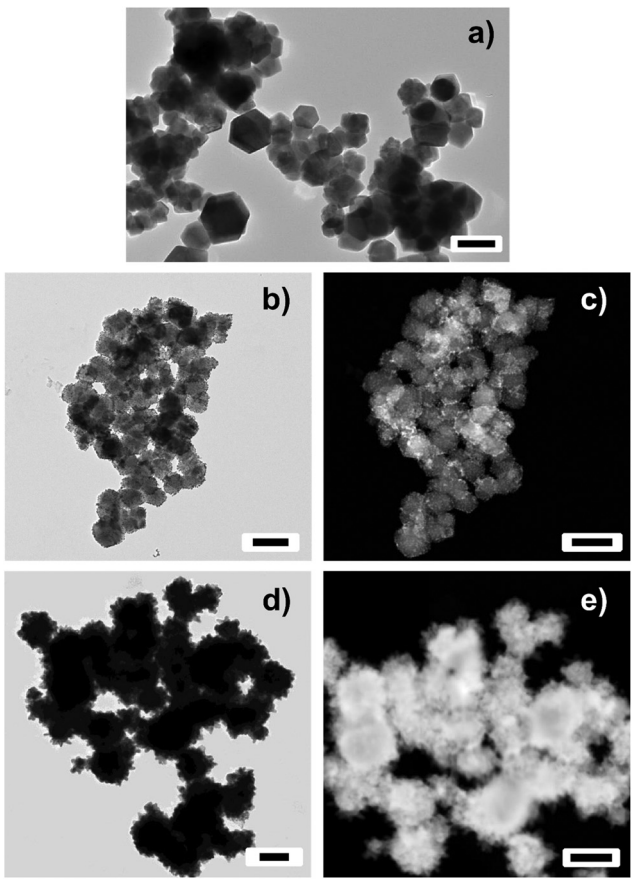

Fig. 1 TEM image of (a) PEI coated Fe_3O_4 (Fe_3O_4–PEI) nanoparticles; (b) bright-field TEM image and (c) corresponding dark-field TEM images of Au seed decorated Fe_3O_4–PEI nanoparticles; (d) bright-field TEM image and (e) corresponding dark-field TEM images of Au-coated Fe_3O_4 (Fe_3O_4@Au) nanoparticles. Scale bars (a), (d) and (e) 100 nm; (b) and (c) 200 nm.

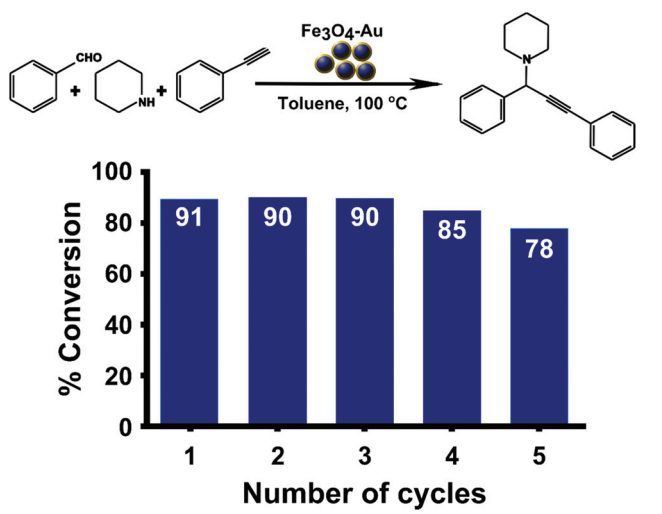

Fig. 2 Recycling of Fe_3O_4@Au nanoparticles catalyst in the A^3-coupling reaction of benzaldehyde, piperidine and phenylacetylene in toluene. Percent conversions were determined by ^{1}H NMR analysis of the crude reaction mixture.

This journal is © The Royal Society of Chemistry 2017

Open Access Article. Published on 17 March 2017. Downloaded on 1/18/2026 6:30:33 PM.
This article is licensed under a Creative Commons Attribution 3.0 Unported Licence.

Table 1 Fe_3O_4@Au nanoparticles catalysed A^3-coupling reaction of aldehydes, piperidine and phenylacetylene, LUMO density and ESP of aldehydes

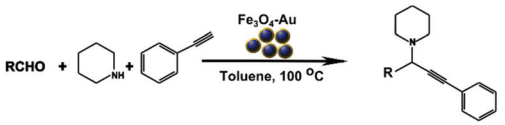

Entry	R	LUMO density[a]	ESP/au[b]	Conversion[c] (%)
1	H	 0.199 au[1]	0.126	95
2	Ph	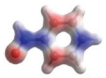 0.139 au[1]	0.103	94
3	1-Naphthyl	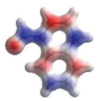 0.108 au[2]	0.099	28
4	4-MeC_6H_4	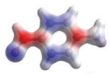 0.136 au[1]	0.099	63
5	4-$MeOC_6H_4$	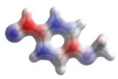 0.138 au[1]	0.094	25
6	4-FC_6H_4	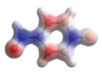 0.137 au[1]	0.106	67
7	4-ClC_6H_4	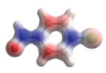 0.131 au[1]	0.111	29
8	3-$NO_2C_6H_4$	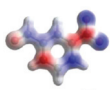 0.050 au[7]	0.122	7
9	2-Furfuryl	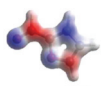 0.139 au[1]	0.102	78
10	2-Thiophenyl	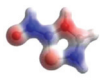 0.126 au[1]	0.102	26
11	2-Pyridyl	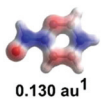 0.130 au[1]	0.108	63

Table 1 *(Contd.)*

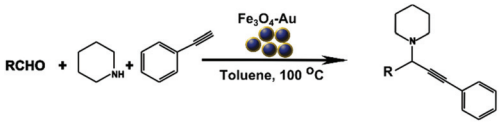

Entry	R	LUMO density[a]	ESP/au[b]	Conversion[c] (%)
12	3-Pyridyl	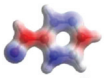 0.130 au[1]	0.114	20
13	4-Pyridyl	 0.132 au[1]	0.119	53

Reaction conditions: aldehyde (1 mmol), piperidine (1 mmol), phenylacetylene (1 mmol) and Fe_3O_4@Au nanoparticales (10 mol%) in toluene (3 mL). [a] LUMO density of carbonyl carbon for aldehydes modelled by B3LYP, 6-311++G (d, p) basis set. Superscript indicates the rank of LUMO associated with carbonyl carbon compared with other atoms in the molecule. [b] Electrostatic potential value of the carbonyl carbon. [c] Conversions determined by ^{1}H NMR of crude reaction mixtures. au, atomic units.

conversion (29%) than 4-fluorobenzaldehyde (67%) (Table 1, entry 6), which could be partly due to the lower electronegativity and larger radius of the Cl atom. 3-Nitrobenzaldehde (Table 1, entry 8) exhibited the lowest conversion (7%), which could be attributed to the presence of the strong electron withdrawing nitro group. For the heterocyclic aldehydes, 2-furaldehyde and 2-thiophenecarboxaldehyde (Table 1, entries 9 and 10 respectively), the latter displayed a lower conversion (26%) which may be due to the lower electronegativity and larger radius of the S atom compared to the O atom. Finally, in the case of the pyridinecarboxaldehydes with nitrogen in the *ortho*, *meta* and *para* positions (Table 1, entries 11, 12 and 13 respectively) displayed a range of conversion rates 63%, 20% and 53%, respectively. This owing to the role of nitrogen as an *ortho*/*para*-director. Herein the electron density is increased in the *meta* position but decreased in the *ortho* and *para* positions *via* resonance effects in the pyridinecarboxaldehyde.

In order to determine the influence of the ESP and LUMO density of the aldehydes in determining the overall conversion, DFT calculations were performed at the B3LYP/6-311++G (d, p) level (Table 1). Since the carbonyl carbons in the aldehydes are more susceptible to nucleophilic addition by piperidine,[31,32] the optimised geometries and LUMO density localised near the carbonyl carbons (electrophilic centres) were evaluated. The propensity of nucleophilic attack may be understood in terms of the localisation of the LUMO at the electrophilic site, which we estimate here as the ESP and LUMO density on the promolecular isoelectron density surface using *CrystalExplorer* software.[33] It is apparent that the ESP is altered with different substituents. For example, benzaldehyde (Table 1, entry 2) has a low ESP (0.103 au) that could be attributed to the weak elec-

Open Access Article. Published on 17 March 2017. Downloaded on 1/18/2026 6:30:33 PM.
This article is licensed under a Creative Commons Attribution 3.0 Unported Licence.

tron-donating properties of benzene (–Ph). In addition, 4-methylbenzaldehyde and 4-methoxybenzaldehyde (Table 1, entries 4 and 5) have comparable ESPs (0.099 and 0.094 au respectively), the lower ESPs compared to benzene may be due to the stronger electron donating effects of the methoxy ($-OCH_3$) and methyl ($-CH_3$) substituents at the *para* position. However, 3-nitrobenzaldehde (Table 1, entry 8) exhibited the highest ESP (0.122 au) which could be attributed to the presence of the strong electron withdrawing nitro group. Accordingly, based on the computational analysis the more electron donating the substituent group is, the lower the ESP at the carbonyl carbon. In addition, the common feature among these different aldehydes is that the majority have the highest LUMO density at carbonyl carbon, indicating that the carbonyl carbon is the favoured position for nucleophilic (piperidine) attack. The two aldehydes that deviate from this trend are 1-naphthaldehyde and 3-nitrobenzaldehyde, which have the 2nd and 7th highest LUMO density respectively at the carbonyl carbon. However, no obvious correlation between conversion and LUMO density as well as ESP was deducible. Therefore, we conclude that in order to fully understand the nature of the reactants and the experimentally observed conversions, it is important to take into account the important role and nature of the nanocatalyst in the calculations. However, due to the limitations of DFT we were unable to incorporate the nanocatalyst in this study.

Finally, we propose a mechanism for the A^3-coupling reaction catalysed by Fe_3O_4@Au nanoparticles (Scheme 1). The reaction is initiated by the coordination of the terminal phenylacetylene to Fe_3O_4@Au nanoparticles to activate the C–H bond. The Au-phenylacetylide intermediate is formed on the surface of the Fe_3O_4@Au nanoparticles, due to the high alkynophilicity of Au metal.[34,35] Meanwhile, the aldehyde and piperidine form the iminium ion *in situ*, which then reacts with the Au-acetylide by nucleophilic addition to give the desired propargylamine and regenerate the active nanoparticle catalyst for further reactions.

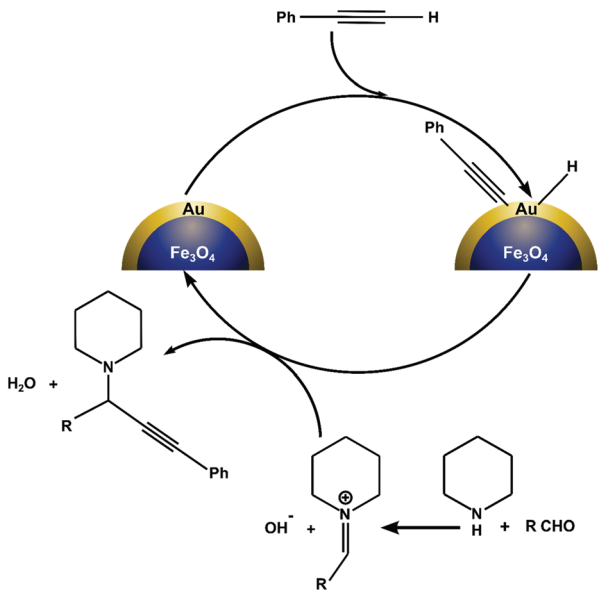

Scheme 1 Schematic illustration of tentative A^3-coupling reaction mechanism catalysed by Fe_3O_4@Au nanoparticles.

In summary, we report a novel magnetically recoverable Fe_3O_4@Au nanocatalyst for the A^3-coupling reaction of aldehydes, amines and alkynes. Under the optimised conditions, various aldehydes produced the corresponding propargylamines with conversions ranging from 7–95%. Importantly, the catalyst could be simply recovered and reused multiple times without significant loss of its catalytic activity. These Fe_3O_4@Au nanoparticles are demonstrated to be a novel and sustainable catalyst for A^3-coupling reactions. Computational analysis of LUMO density and ESP calculations were carried out using DFT. The majority of aldehydes displayed high LUMO density at carbonyl carbon, confirming that the carbonyl carbon is the favoured position for nucleophilic addition. The ESP is altered with different substituents, aldehydes with stronger electron donating substituents displayed lower ESP values while those with stronger electron withdrawing substituents displayed higher ESP values. However, no correlation was obtained between calculated LUMO density, ESP values and experimental percent conversions. Finally, this study establishes that the size and shape dependent properties of Fe_3O_4@Au nanoparticles should be further explored to better determine the catalyst efficiency in various carbon–heteroatom coupling reactions to produce C–O, C–S and C–N bonds.

Conflict of interest

The authors declare no competing financial interests.

Acknowledgements

The authors acknowledge the Australian Microscopy & Microanalysis Research Facility at the Centre for Microscopy, Characterization & Analysis, The University of Western Australia, funded by the University, State and Commonwealth Governments. A. M. Munshi would like to thank Umm Al-Qura University, Makkah, Saudi Arabia for a postgraduate scholarship. Support of the work from the Australian Research Council and The Perth Mint is also acknowledged.

Notes and references

1 M. A. Huffman, N. Yasuda, A. E. DeCamp and E. J. J. Grabowski, *J. Org. Chem.*, 1995, **60**, 1590–1594.
2 M. Miura, M. Enna, K. Okuro and M. Nomura, *J. Org. Chem.*, 1995, **60**, 4999–5004.
3 G. Dyker, *Angew. Chem., Int. Ed.*, 1999, **38**, 1698–1712.
4 M. E. Jung and A. Huang, *Org. Lett.*, 2000, **2**, 2659–2661.
5 T. Murai, Y. Mutoh, Y. Ohta and M. Murakami, *J. Am. Chem. Soc.*, 2004, **126**, 5968–5969.

 This journal is © The Royal Society of Chemistry 2017

Open Access Article. Published on 17 March 2017. Downloaded on 1/18/2026 6:30:33 PM.
This article is licensed under a Creative Commons Attribution 3.0 Unported Licence.

6 V. K.-Y. Lo, Y. Liu, M.-K. Wong and C.-M. Che, *Org. Lett.*, 2006, **8**, 1529–1532.
7 C. Wei and C.-J. Li, *J. Am. Chem. Soc.*, 2003, **125**, 9584–9585.
8 L. Shi, Y.-Q. Tu, M. Wang, F.-M. Zhang and C.-A. Fan, *Org. Lett.*, 2004, **6**, 1001–1003.
9 C. Fischer and E. M. Carreira, *Org. Lett.*, 2001, **3**, 4319–4321.
10 C. Wei, Z. Li and C.-J. Li, *Org. Lett.*, 2003, **5**, 4473–4475.
11 W.-W. Chen, R. V. Nguyen and C.-J. Li, *Tetrahedron Lett.*, 2009, **50**, 2895–2898.
12 V. Polshettiwar and R. S. Varma, *Green Chem.*, 2010, **12**, 743–754.
13 V. Polshettiwar, T. Asefa and G. Hutchings, *Nanocatalysis: Synthesis and Applications*, Wiley, 2013.
14 R. J. White, R. Luque, V. L. Budarin, J. H. Clark and D. J. Macquarrie, *Chem. Soc. Rev.*, 2009, **38**, 481–494.
15 J. M. Campelo, D. Luna, R. Luque, J. M. Marinas and A. A. Romero, *ChemSusChem*, 2009, **2**, 18–45.
16 B. Karimi, M. Gholinejad and M. Khorasani, *Chem. Commun.*, 2012, **48**, 8961–8963.
17 M. Kidwai, V. Bansal, A. Kumar and S. Mozumdar, *Green Chem.*, 2007, **9**, 742–745.
18 K. K. R. Datta, B. V. S. Reddy, K. Ariga and A. Vinu, *Angew. Chem., Int. Ed.*, 2010, **49**, 5961–5965.
19 L. Abahmane, J. M. Köhler and G. A. Groß, *Chem. – Eur. J.*, 2011, **17**, 3005–3010.
20 T. Zeng, W.-W. Chen, C. M. Cirtiu, A. Moores, G. Song and C.-J. Li, *Green Chem.*, 2010, **12**, 570–573.
21 S. Shylesh, V. Schünemann and W. R. Thiel, *Angew. Chem., Int. Ed.*, 2010, **49**, 3428–3459.
22 S. H. Joo, J. Y. Park, C.-K. Tsung, Y. Yamada, P. Yang and G. A. Somorjai, *Nat. Mater.*, 2009, **8**, 126–131.
23 J. Qi, J. Chen, G. Li, S. Li, Y. Gao and Z. Tang, *Energy Environ. Sci.*, 2012, **5**, 8937–8941.
24 J. C. Park and H. Song, *Nano Res.*, 2011, **4**, 33–49.
25 J. Lee, J. C. Park and H. Song, *Adv. Mater.*, 2008, **20**, 1523–1528.
26 W. Jiang, Y. Zhou, Y. Zhang, S. Xuan and X. Gong, *Dalton Trans.*, 2012, **41**, 4594–4601.
27 F. Mi, X. Chen, Y. Ma, S. Yin, F. Yuan and H. Zhang, *Chem. Commun.*, 2011, **47**, 12804–12806.
28 Y. Zhao, Y. Yeh, R. Liu, J. You and F. Qu, *Solid State Sci.*, 2015, **45**, 9–14.
29 I. Y. Goon, L. M. H. Lai, M. Lim, P. Munroe, J. J. Gooding and R. Amal, *Chem. Mater.*, 2009, **21**, 673–681.
30 A. M. Munshi, V. Agarwal, D. Ho, C. L. Raston, M. Saunders, N. M. Smith and K. S. Iyer, *Cryst. Growth Des.*, 2016, **16**, 4773–4776.
31 R. Krishnan, J. S. Binkley, R. Seeger and J. A. Pople, *J. Chem. Phys.*, 1980, **72**, 650–654.
32 M. J. Frisch, J. A. Pople and J. S. Binkley, *J. Chem. Phys.*, 1984, **80**, 3265–3269.
33 M. J. Turner, J. J. McKinnon, S. K. Wolff, D. J. Grimwood, P. R. Spackman, D. Jayatilaka and M. A. Spackman, *Crystal Explorer17*, University of Western Australia, 2017, http://hirshfeldsurface.net.
34 C.-J. Li, *Acc. Chem. Res.*, 2010, **43**, 581–590.
35 X. Zhang and A. Corma, *Angew. Chem., Int. Ed.*, 2008, **47**, 4358–4361.